Available online at www.sciencedirect.com

SCIENCE DIRECT®

Journal of Controlled Release 108 (2005) 193–214

journal of controlled release

www.elsevier.com/locate/jconrel

Targeted nanoparticles for drug delivery through the blood–brain barrier for Alzheimer's disease☆

Celeste Roney [a], Padmakar Kulkarni [a], Veera Arora [a], Peter Antich [a], Frederick Bonte [a], Aimei Wu [b], N.N. Mallikarjuana [b], Sanjeev Manohar [b], Hsiang-Fa Liang [c], Anandrao R. Kulkarni [c], Hsing-Wen Sung [c], Malladi Sairam [d], Tejraj M. Aminabhavi [d,*]

[a] *Department of Radiology, Division of Advanced Radiological Sciences, The University of Texas Southwestern Medical Center at Dallas, Dallas, TX 75390, United States*

[b] *Alan G. MacDiarmid Laboratory for Scientific Innovation, Department of Chemistry, The University of Texas at Dallas, Richardson, TX 75083, United States*

[c] *Department of Chemical Engineering, National Tsing Hua University, Hsinchu, Taiwan 30013, ROC*

[d] *Drug Delivery Division, Center of Excellence in Polymer Science, Karnatak University, Dharwad, 580 003, India*

Received 7 March 2005; accepted 24 July 2005
Available online 24 October 2005

Abstract

Alzheimer's disease (AD) is the most common cause of dementia among the elderly, affecting 5% of Americans over age 65, and 20% over age 80. An excess of senile plaques (β-amyloid protein) and neurofibrillary tangles (tau protein), ventricular enlargement, and cortical atrophy characterizes it. Unfortunately, targeted drug delivery to the central nervous system (CNS), for the therapeutic advancement of neurodegenerative disorders such as Alzheimer's, is complicated by restrictive mechanisms imposed at the blood–brain barrier (BBB). Opsonization by plasma proteins in the systemic circulation is an additional impediment to cerebral drug delivery. This review gives an account of the BBB and discusses the literature on biodegradable polymeric nanoparticles (NPs) with appropriate surface modifications that can deliver drugs of interest beyond the BBB for diagnostic and therapeutic applications in neurological disorders, such as AD. The physicochemical properties of the NPs at different surfactant concentrations, stabilizers, and amyloid-affinity agents could influence the transport mechanism.

Keywords: Blood–brain barrier; Alzheimer's disease; Nanoparticles; Targeted drug delivery; Central nervous system

☆ This article is CEPS communication # 67.

* Corresponding author. Fax: +91 836 2771275.
E-mail address: aminabhavi@yahoo.com (T.M. Aminabhavi).

0168-3659/$ - see front matter © 2005 Elsevier B.V. All rights reserved.
doi:10.1016/j.jconrel.2005.07.024

Contents

1. Introduction

Alzheimer's disease (AD), a neurodegenerative disorder of the elderly, is the most prevalent form of dementia. The cognitive decline associated with AD drastically affects the social and behavioral skills of people living with this disease. Notwithstanding the social impact, however, AD also imparts great financial burdens on patients, families, and the community as a whole. The National Institutes of Health (NIH) estimates that 4.5 million Americans are affected by AD, at an annual cost of $100 billion per year. Yet even more ominous is the estimate that by 2050, 13.2 million older Americans are expected to have AD if the current trends hold and no preventive treatment becomes available. These statistics are exacerbated by the fact that there are no current biological markers of AD, and therefore, definitive diagnoses are made upon autopsy and new treatment efficacy cannot be extended overtime. Furthermore, therapeutic strategies to probe the central nervous system (CNS) are limited by the restrictive tight junctions at the endothelial cells of the blood–brain barrier (BBB). To overcome the impositions of the BBB, polymeric biocompatible drug carriers have been applied to the central nervous system for many applications such as cancers, but the field of nanoparticulate drug carrier technology is not well developed in AD research [1]. Polymeric nanoparticles are promising candidates in the investigation of AD because nanoparticles are capable of: opening tight junctions [2] crossing the BBB [3], high drug loading capacities, targeting towards the mutagenic proteins of Alzheimer's [4,5]. The present review gives an account of BBB and discusses the literature on biodegradable polymeric nanoparticles (NPs) with appropriate surface modifications that can deliver drugs of interest beyond the BBB for diagnostic and therapeutic applications in neurological disorders, particularly AD.

2. Blood–brain barrier

The blood–brain barrier (BBB) is the homeostatic defense mechanism of the brain against pathogens and

toxins. Complex and highly regulated, the BBB screens the biochemical, physicochemical and structural features of solutes at its periphery, thus affording barrier selectivity in the passage of desired molecules into the brain parenchyma. Early revelations of the BBB illustrated its biological character in the murine model, and provided insights into contemporary understandings of its physiology. Electron microscopic analyses of isolated cerebral cortices, post intravenous injection of the enzymatic tracer horseradish peroxidase (HRP), exposed the presence of exogenous HRP in the vascular space and in endothelial cell pinocytotic vacuoles [6]. The pinocytotic vacuoles were not found to transport the enzyme, and furthermore, no peroxidase was found beyond the vasculature endothelium, suggesting a "barrier" between the blood and the brain.

2.1. Biology of the BBB

Cerebral capillaries are created by the process of angiogenesis, which is the development of blood vessels from those existing in previously formed complexes. Fig. 1 shows a depiction of the cerebral capillaries, while the features of the BBB are exhibited in Fig. 2. During angiogenesis, endothelial cells (EC)

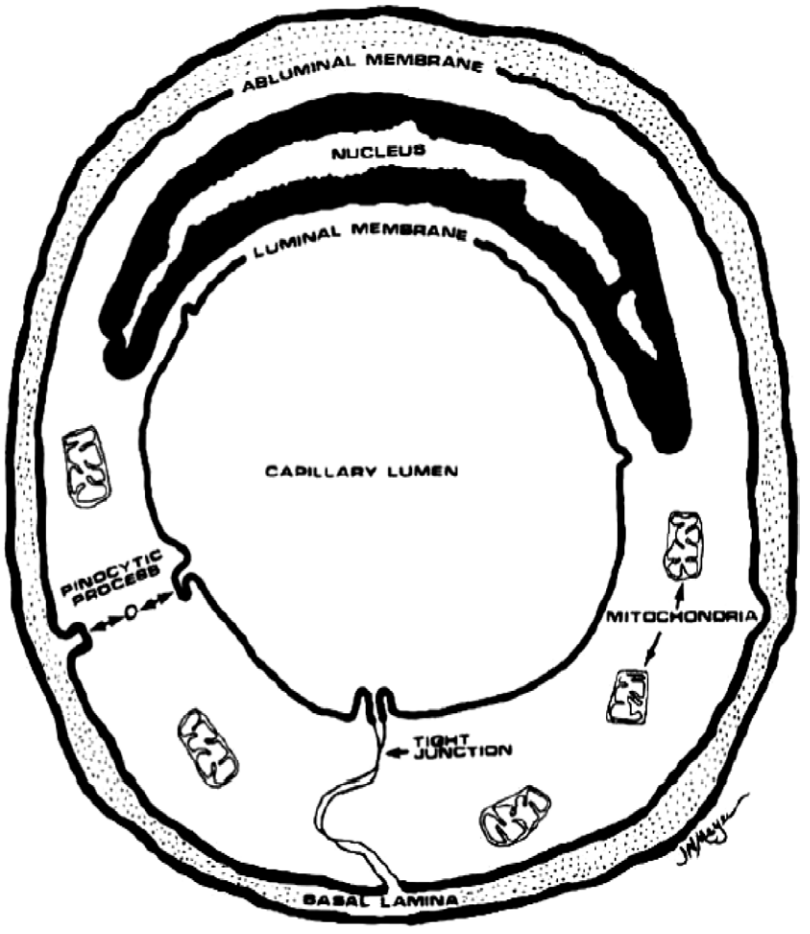

Fig. 1. Characteristic features of BBB are represented in this schematic diagram of a cerebral capillary viz., tight junctions and scarcity of pinocytic vacuoles. Note the presence of mitochondria, which are denser in cerebral EC as compared to peripheral EC. This may be attributed to extra metabolic workload required to maintain ionic gradients at BBB (figure taken from: Burns E., Dobben G., Kruckeberg T., Gaetano P., Blood–brain barrier: Morphology, physiology, and effects of contrast media, Adv. Neurol., 30, (1981) 159–165, Carney A. Ed., Raven Press NY).

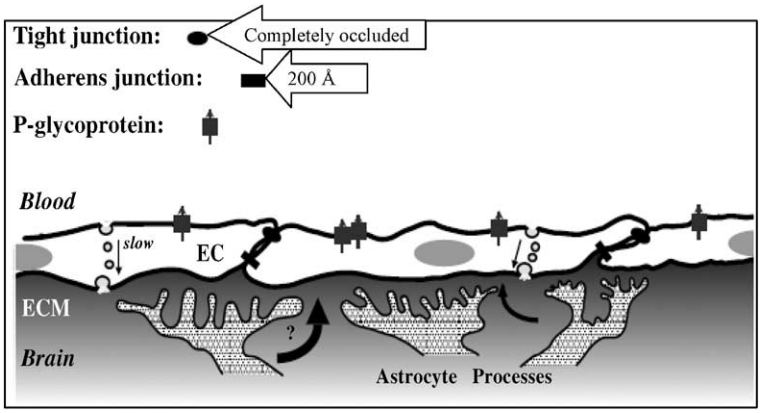

Fig. 2. Features of BBB. The endothelial cells (EC) of BBB are coupled by tight junctions (TJ) that are completely occluded and adherens junctions (200 Å). The increased electrical resistance at the TJ strains paracellular movement of substances into the brain. Proteins of the adherens junction work in accordance with TJ proteins for cellular adherence. Astrocytic processes (glial cells) in the extracellular matrix (ECM) envelope the capillaries and influence transport across the EC. Questions once arose as to whether or not astrocytes actually participated in BBB. It is now accepted that 20 nm gap between adjacent astrocytes supports that they do not. P-glycoproteins (P-gp) on apical EC membrane efflux substances from brain into bloodstream (reprinted with permission from Annual Review of Neuroscience, Vol. 22 (1999) by Annual Reviews www.annualreviews.org).

traverse the extracellular matrix (ECM) and degrade the basement membrane to create a microvascular network [6,7] thus subsequent proliferation. Proliferation of endothelial cells is influenced by neural determinants. These confer the characteristic physiological properties upon the BBB, and consequently, cerebral EC are distinguished from the EC of the periphery. For instance, the brain EC have fewer endocytotic vessels than peripheral EC, which limits the transcellular flux at the BBB. The occluded tight junctions, whose great electrical resistance imposes barriers to paracellular flux, join endothelial cells of the brain. The structural properties of cerebral EC, mentioned above, help to define the selectiveness at the BBB. Furthermore, cerebral EC have more mitochondria [7] than peripheral EC, which drives the increased metabolic workload necessary to maintain ionic gradients across the BBB.

The electron-dense layers of the basement membrane fuse EC and astrocytes, while dividing EC and pericytes from the surrounding extracellular space. Pericytes lie along the outer axes of cerebral capillaries and perform in contractility. This close association (and function) helps to monitor blood flow, and thus, the adhesion of pericytes with the microvasculature indirectly regulates EC activity and BBB transport. Pericytes could also manage endothelial growth and development by inhibiting cell proliferation [8], and in a contrasted dual role, by contributing to angiogenesis [9].

Astrocytes envelop more than 99% of the basal capillary membrane [10], and they also play a role in the BBB induction of high paracellular electrical resistance. A gap of only 20 nm separates the astrocytes from the EC and the pericytes. Likewise, the significant interplay amongst the three cells contributes to the solute transportation. Namely, molecular route into the brain (from the blood) is first accomplished by moving beyond the astrocytic processes and then by moving through the immediate perivascular spaces, and onto the pericytes bordering the capillaries. Consequentially, transporters, receptors and enzymes located on the plasma membranes of astrocytes and pericytes govern the fates of solutes before they reach the EC [10,11].

2.2. Molecular physiology of the BBB

The BBB restricts solute entry into the brain, by the transcellular route, due to an increased electrical resistance between the endothelial cells at the tight junctions (TJ). The intact BBB exhibits estimated electrical resistances up to 8000 Ω/cm^2, whereas leaky endothelia demonstrates the resistances between 100 and 200 Ω/cm^2 [12–14]. Key indispensable

proteins, including claudin 1-, 3-, and 5-, occludin and the junctional adhesion molecule (JAM), compose the tight junction [15–19]. The claudins form the seal of the TJ by homotypically binding to each other on adjacent EC cells. In an interesting review of the pathophysiology of tight junctions, Mitic et al. provide convincing evidence for the role of claudins in fibrilizing and forming the TJ seal [20]. However, the claudins are not the sole components of the fibrils; this role being shared with occludin. In addition, the occludin protein directs the BBB to decrease paracellular permeability by localizing into intramembrane strands of the TJ [21]; the number of localized proteins parallels the impedance to solute flux [22]. Meanwhile, the JAM regulates leukocyte transmigration at the BBB [18]. Of particular interest, leukocyte passage instigates BBB compromise [7]. As well, a host of other transmembrane proteins lie in accessory to the three integral proteins [20]. According to Reichel et al., the expression of complex tight junctions between the ECs is one of the most critical features because of their consequences on the function of the BBB [23]: (i) nearly complete restriction of the paracellular pathway, (ii) enforcement of transendothelial passage and hence, control over the CNS penetration, (iii) association with expression of specific carrier systems for hydrophilic solutes essential for the brain (e.g. nutrients), and (iv) differential (i.e. polarized) expression of receptors, transporters, and enzymes at either the luminal or abluminal cell surface allowing the BBB to act as a truly dynamic interface between the body periphery (blood) and the central compartment (brain).

2.3. BBB breakdown and mechanisms of disease

Decomposition of the BBB occurs in response to initiators such as infection (e.g. bacterial, viral), inflammation, cerebrovascular disease, and neoplasia. Motivators of BBB breakdown augment permeability, and underlie a myriad of neuropathologies. In pneumonia, the pneumococcus bacterium joins the BBB via platelet activating factor receptors [24]. The outcome of bacterial adhesion is an increased vesicular transport across the endothelial cells, thus permitting separation of the tight junctions, and creating an entry for inflammatory peptides. Likewise, infection of the brain space ensues. The consistency of the BBB is also influenced by the actions causing bacterial meningitis. The meningococcus bacterium [25] enters the body through the nose, and thereafter infiltrates the endothelia (via the pili) of the cerebrum to cause infection of the CNS [25]. Viral invasions of the CNS pronounce less impairment to the BBB than do bacterial interferences, and therefore, the integrity of the BBB is upheld to a greater extent following the viral attack [26]. Inflammatory stimuli such as pain induce the extravasation of lymphoid cells through the BBB [27], opening the barrier to cytokines and chemokines, and resulting in autoimmune inflammatory disorders like multiple sclerosis (MS) and CNS lupus. In addition, the BBB can be compromised in cerebrovascular disease, for example stroke, by hypertension and ischemia. Ischemia complicates the disease progression by activating cytokines and proteases [26].

As previously mentioned, degradation of the BBB occurs in states of pathology, such as hypertension, ischemia, and hydrocephalus or in cases of trauma. The various factors involved in the BBB breakdown and homeostasis are compiled in Table 1. Degradation leads to leakiness and the consequential unrestrained migration of malicious agents into the cerebrum. In addition to existing pathological conditions, and even in the intact BBB, crucial parameters must be regarded when ascertaining the capabilities of molecules to cross the BBB, especially for the intended purpose of drug design. The implication is that targeted, controlled drug delivery through the BBB, would promote a greater understanding at the molecular level of many unfathomable neurological disorders, as well as aid in their early diagnoses, and their therapeutic advancements.

Table 1
BBB degradation and homeostatic organs

Causes of BBB degradation	BBB homeostatic organs	Focus of homeostatic regulation
Hypertension	Pineal gland	Circadian rhythm
Abnormal development	Neurohypophysis	Posterior pituitary hormones
Microwaves	Area postrema	Vomiting reflex
Radiation	Subfornical organ	Bodily fluids
Infection	Lamina terminalis	Chemosensory
Trauma	Median eminance	Anterior pituitary hormones

2.4. Drug transport to the barrier and targeting mechanisms

The BBB is circumferential, formed by the polarized luminal (apical) and abluminal (basal) endothelial membranes (and other tissue [3] interfaces not mentioned in this review), which lie in series. Thus, solutes have to pass a set of membranes to gain brain entry, making the BBB dynamic in its regulation. The barrier uptakes essential nutrients, hormones and vitamins, while enzymatically degrading many peptides and neurotransmitters through enzymatic BBB. Additionally, the energy-requiring toxin efflux mechanisms help to maintain cerebral vitality by disavowing injurious substances. Kinetic flux analyses reveal a unidirectional, concentration-dependent movement of the solutes [28]. Furthermore, the direction of flow is from the plasma to the brain, or visa versa, with these two parameters defining influx and efflux (see Fig. 3).

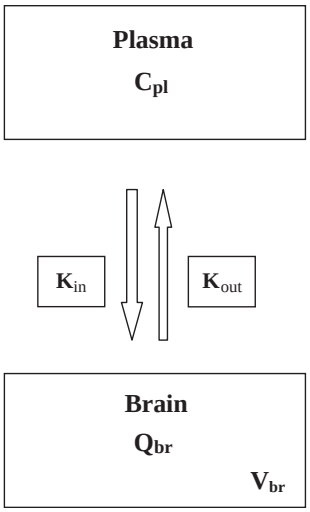

Fig. 3. Schematic representation of unidirectional, concentration-dependant solute flux. The transfer coefficient, K, quantifies the rates of influx (K_{in}) and efflux (K_{out}) at the BBB, which rely on solute concentrations in blood plasma (C_{pl}) in the brain. The concentration of the solute in the brain is represented as Q_{br}, which describes the quantity (Q) of the solute/gram wt of the brain tissue. The concentration of solute in the brain is determined by the brain volume of distribution (V_{br}) as: $C_{br}=Q_{br}/V_{br}$. Even though these specific quantitative variables are not explicitly stated in the text, the importance of BBB flux to drug delivery is important (reprinted with permission from Q. Smith, A review of blood–brain barrier transport techniques, From: Methods in Molecular Medicine: The Blood Brain Barrier: Biology and Research Protocols, Ed. by S. Nag, Humana Press Inc., Totowa, NJ, 89 (2003) 193–205).

Thus, net flux is the difference between the two unidirectional rates, and is greatly influenced by the nature of the BBB. Importantly, BBB flux is a determinant in drugs reaching therapeutic concentrations within the CNS [29]. Numerous transport mechanisms define the BBB (see Fig. 4). Small lipophilic molecules most easily pass from the capillaries. Those molecules that are charge bearing, large or hydrophilic, require gated channels, ATP, proteins and/or receptors, to facilitate passage through the BBB. One exceptional regulatory aspect of the BBB is that it is not fully present throughout the brain. The circumventricular organs, which border the ventricles of the brain, do not possess a BBB. These organs are concerned with chemosensation, hormonal adjustment (from the autonomic nervous system), circadian rhythm, vomiting and the regulation of bodily fluids. The absence of a BBB at these checkpoint organs encourages the maintenance of a constant cerebral internal atmosphere by monitoring the blood make-up and activating feedback controls as necessary.

Transport mechanisms at the BBB can be manipulated for cerebral drug targeting. Naturally, ideal drug candidates should be small, lipophilic (as measured by the octanol: water partition coefficient), hydrophobic, and compact (a parameter measured by the polar surface area). Physicochemical factors notwithstanding, though, the nature of the drug candidate within the biological system is paramount to the drug design. In the peripheral circulation, systemic enzymatic attack and plasma protein opsonization can lead to the metabolism of the drug before it reaches the brain. The factors influencing drug transport into the brain are given in Table 2. Moreover, the probability of cellular sequestration and the clearance rate of the drug in the bloodstream are additional issues to consider in drug targeting. Finally, an understanding of the clearance rate of the candidate drug in the brain is imperative, and as such, focus should be given to the concentration of the drug in the brain, with respect to the concentration of the drug in the blood, called the log BB. While designing the drug, it is extremely important to consider several parameters such as drug concentration, lipophilicity, and polar surface area. Efflux proteins and other obstacles at the BBB must be surmounted before the drug reaches the interior of the brain.

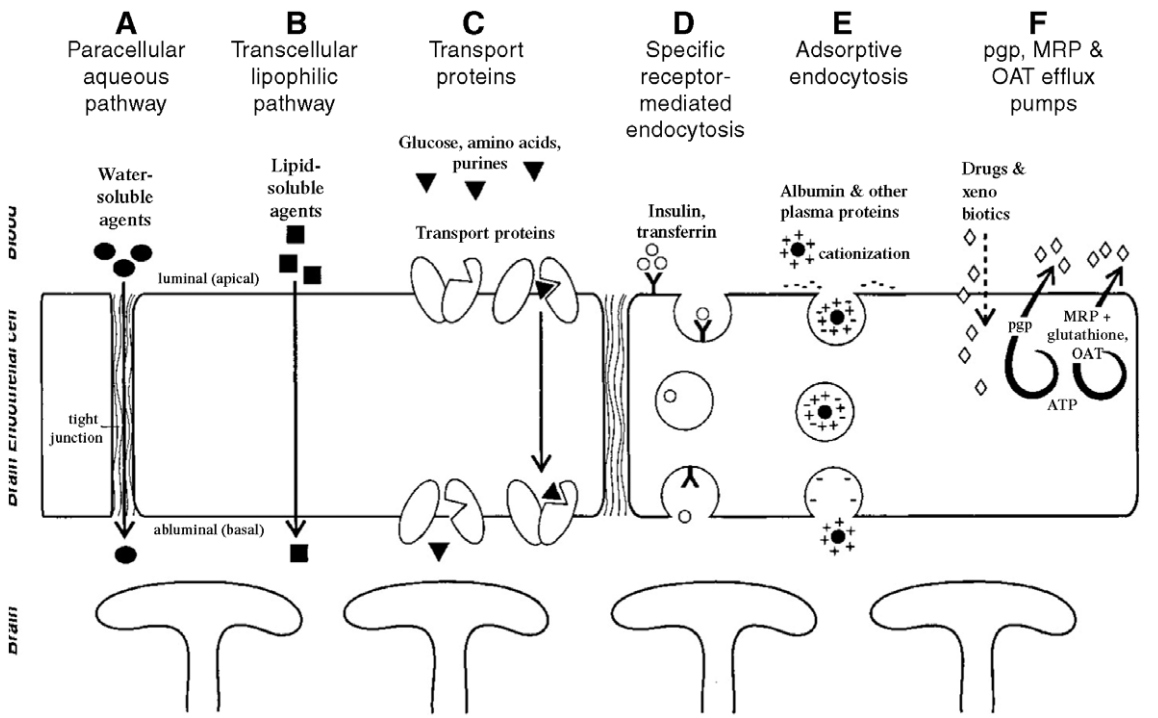

Fig. 4. Transport mechanisms at the BBB (reprinted with permission from E. Neuwelt, Mechanism of disease: The blood–brain barrier, Neurosurgery, 54 (2004) 131–141).

At the endothelial cell membrane, the drug can proceed through a variety of routes. In a hypothetical situation, considering all drug molecules as the same (which are being defined as Drug A, Drug B, and Drug C), Drug A attaches to the basal EC membrane (see Fig. 5). If Drug A has an affinity for efflux proteins at the BBB, it is shuttled back into the bloodstream without reaching its goal. If there is no affinity for efflux proteins, Drug A settles into the internal compartment of the EC cell where it faces the chances of encountering metabolic cellular enzymes, again jeopardizing its likelihood of reaching the target site. Assuming that Drug A hurdles all obstacles imposed by efflux proteins and cellular enzymes, it then proceeds through the cell, to the apical EC membrane, and into the brain towards its target. Drug A in the extracellular space (ECS) may proceed by different paths to reach its objective. It can leave the ECS before reaching its destination, travel directly to its target, or it may act like Drug B, traveling to its target via the cerebrospinal fluid (CSF). If Drug A leaves the ECS, its fate becomes that of the peripheral circulation and the actions of serum enzymes. Additionally, Drugs A and B may be in equilibrium between the CSF and the ECS, between the CSF and the target cell, and between the target cell and the ECS. In the peripheral circulation, Drug C equilibrates with red

Table 2
Considerations for drug transport into the brain

Factors at the BBB	Peripheral factors
Concentration gradients of drug/polymer	Systemic enzymatic stability
Molecular weight (of drug)	Affinity for plasma proteins
Flexibility, conformation of drug/polymer	Cerebral blood flow
Amino acid composition	Metabolism by other tissues
Lipophilicity	Clearance rate of drug/polymer
Sequestration by other cells	Effects of existing pathological conditions
Affinity for efflux proteins (e.g. P-gp)	
Cellular enzymatic stability	
Existing pathological conditions	
Molecular charge (of drug/polymer)	
Affinity for receptors or carriers	

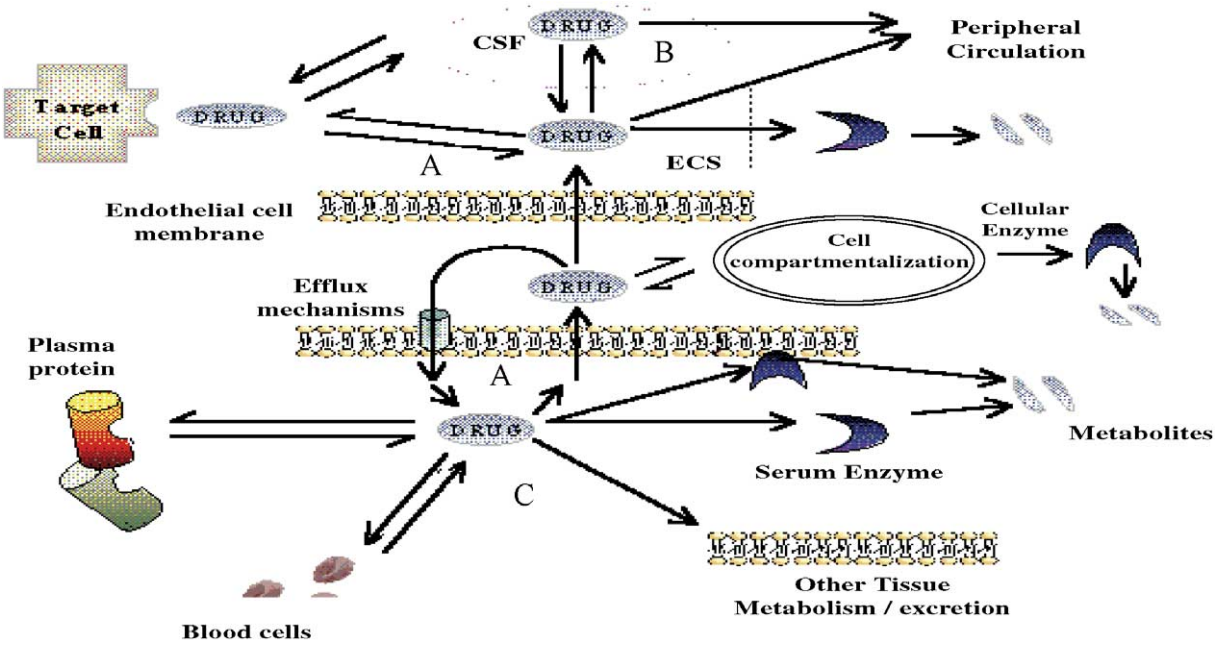

Fig. 5. Mechanism of drug transport and delivery. Hypothetical Drugs A, B and C (adopted from http://users.ahsc.arizona.edu/davis/transport2.htm).

blood cells (RBC) and plasma proteins. Plasma proteins can attach to the surface of Drug C, making it more amenable for macrophage uptake by the liver and spleen, and therefore, less likely to reach the brain. As previously mentioned, Drug C can also be metabolized by serum enzymes or it can be taken up by systemic tissues and metabolized, never to reach the targeted cells of the brain.

Two basic paradigms in cerebral drug targeting are found for the molecular approach and the polymeric carrier approach. By the molecular approach, two further schemes can be probed. First, drugs can be targeted to the brain cells (based upon the vital determinants such as lipophilicity, size and polar surface area) and then activated once inside the target cell by the specific enzymatic machinery. The disadvantage to this tactic, though, is the limited availability of such drugs and metabolic pathways for potential exploitation. Also, by the molecular approach, candidate drugs can be targeted to the BBB via receptor-mediation. However, receptor targeted moieties face additional challenges. In particular, many receptors are not specific to only one cell type. Thus, candidate drugs may have an affinity for cells other than their intended targets. The second major paradigm in cerebral drug targeting is by using particulate carriers. Examples of particulate carriers are liposomes, oil-in-water (O/W) emulsions, and polymeric nanoparticles.

Polymeric nanoparticles are advantageous in a number of ways. For one, they possess the high drug-loading capacities, thereby increasing intracellular delivery of the drug. Secondly, the solid matrix of particulate carriers protects the incorporated drugs against degradation, thus increasing the chances of the drug reaching the brain. Furthermore, carriers can target delivery of drugs, and this targeted delivery can be controlled. One additional benefit of particulate carriers is that their surface properties can be manipulated in such a way as to evade recognition by the macrophages of the reticuloendothelial system (RES), hence improving the likelihood of nanoparticles reaching the brain. Kabanov and Batrakova [30] gave an interesting review of maximizing drug transport through the BBB by inhibiting efflux transporters by block copolymers, by using artificial hydrophobitization of peptides and proteins by fatty acids, and by using receptor-mediated drug encapsulated nanoparticles [30].

3. Polymeric nanoparticles

One potential in delivering drugs to the brain is the employment of nanoparticles. Nanoparticles are polymeric particles made of natural or artificial polymers ranging in size between 10 and 1000 nm (1 μm) [31]. Compared with other colloidal carriers, polymeric nanoparticles present a higher stability when in contact with the biological fluids. Also, their polymeric nature permits the attainment of desired properties such as controlled and sustained drug release. Different approaches in the fabrication of nanoparticles consisting of biodegradable polymers have been described. Likewise, methods for the preparation of surface-modified sterically stabilized particles are reviewed in the literature [32–46].

Nanoparticles can be synthesized from preformed polymers or from a monomer during its polymerization, as in the case of alkylcyanoacrylates. As such, nanospheres or nanocapsules can be synthesized, with their resultant structures that are dependent upon the technology employed in the manufacture. Nanospheres are the dense polymeric matrices in which drug is dispersed, whereas nanocapsules present a liquid core surrounded by a polymeric shell. Most techniques involving the polymerization of monomers include the addition of the monomer into the dispersed phase of an emulsion, an inverse microemulsion or dissolved into a non-solvent of the polymer [32–46]. Starting from the preformed polymers, nanoparticles are formed by the precipitation of synthetic polymers or by denaturation or gelification of natural macromolecules [31,34–36,38,39,41–44,46]. Finally, two main approaches have been proposed for the preparation of nanoparticles by synthetic polymers. The theory of the first scheme follows the emulsification of a water-immiscible organic solution of the polymer, in a surfactant-containing aqueous phase, and followed by solvent evaporation. The second approach follows the precipitation of a polymer after the addition of a non-solvent of the polymer.

Thus far, the only successfully used nanoparticles for the in vivo administration of drugs targeted to the brain, is the rapidly biodegradable polybutylcyanoacrylate (PBCA) [47]. The mechanism of emulsion polymerization of polyalkylcyanoacrylates (PACA) is represented in Fig. 6. Kreuter et al. have suggested that the passage of PBCA nanoparticles through the

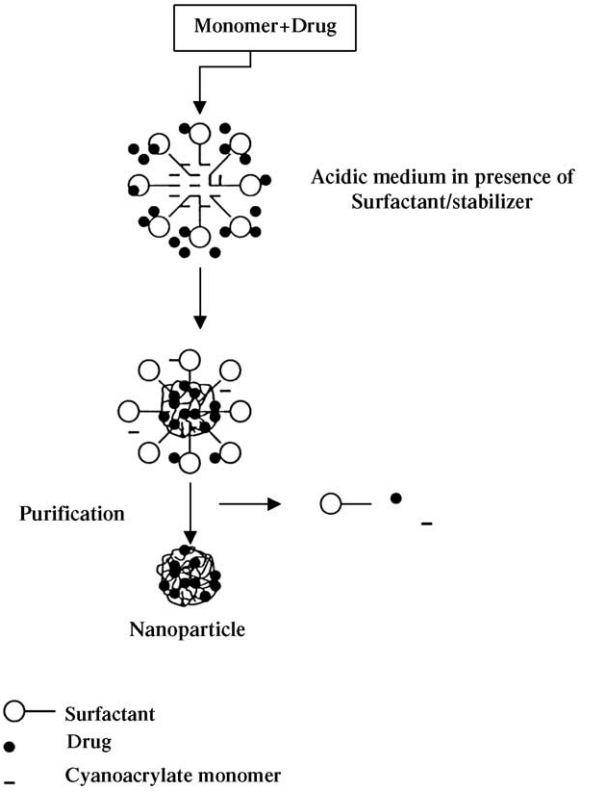

Fig. 6. Emulsion polymerization of alkylcyanoacrylates (reprinted from J. Control. Rel. 70 (2001)1–20, 2001, K.S. Soppimath, A.R. Kulkarni, W.E. Rudziniski, T.M. Aminabhavi, Biodegradable polymeric nanoparticles as drug delivery devices, with permission from Elsevier).

BBB probably occurs by phagocytosis or endocytosis by the endothelial cells [48]. Schroeder et al. [49] replicated the work of Kreuter et al. [48]. Schroeder et al. further points to a model of diffusion of the NPs at the BBB [50]. Vauthier et al. refutes endocytosis as the mechanism for EC uptake of PACA, and suggests NP adherence to the cell membrane with subsequent escape by the P-gp efflux proteins [51].

3.1. Production of nanoparticles by different techniques

3.1.1. Emulsion polymerization

The anionic polymerization of alkylcyanoacrylate monomers into polymeric NPs follows the emulsion polymerization technique. By this method, the monomer is dispersed in aqueous solution as a uniform emulsion and stabilized by the surfactants. The sur-

factants facilitate emulsification of the monomer into the aqueous phase by decreasing surface tension at the monomer–water interface. Dispersion of the surfactant persists until the critical micellar concentration (CMC) is realized. The CMC is the concentration beyond which the surfactant no longer exists as a soluble dispersion, but rather as molecular aggregates called micelles [52]. Henceforth, equilibrium is maintained between the dispersed surfactant molecules and the micelles. Beyond the CMC, only micellar formation is possible.

Micelles contain both polar and non-polar ends. They aggregate with the polar heads lying outwards, allowing the nonpolar hydrocarbons to form the interior, where the monomer is solubilized. Upon addition of the monomer, and with agitation, emulsification commences. Typically, water-soluble initiators are used in emulsions. The system contains monomer droplets in the aqueous phase, and the solubilized monomer in the interior of the micelle. With water-soluble initiators, chain growth starts at the surface of the micelle, it being hydrophilic. Once the monomer inside the micelle is expended, more droplets enter from the aqueous phase. Thus, polymerization proceeds inwards and continues until prohibited by free-radical termination. Many polymer chains grow within the system and eventually aggregate into fine particles. The emulsifier layer of the micelle stabilizes these particles until the micelle bursts, releasing the particles. Nanoparticles are uniformly dispersed in the aqueous phase, and stabilized by the emulsion molecules, which originally formed the micelle [52].

3.1.2. Dispersion polymerization

Gubha and Mandal have prepared the NPs of polyacrylamide (PAM) by the dispersion polymerization of acrylamide monomer at 40 °C [36]. They used the partial isopropyl ester derivative of poly(vinyl methyl ether-*alt*-maleicanhydride) (PVME-alt-MA), called PVME-*co*-MA-*co*-iPrMA, as the stabilizer, and ammonium persulfate (APS) as the initiator. In *t*-butyl alcohol (TBA)–water media, they achieved successful polymerization at an alcohol concentration of 90%. However, it was found that if the maleic anhydride groups are not converted to monoisopropyl ester in PVME-*alt*-MA (i.e. using PVME-*alt*-MA as opposed to PVME-*co*-MA-*co*-iPrMA), then the NPs coagulate in acetone upon isolation, suggesting that the stabilizer detaches from the surface of the particles upon centrifugation. The stabilizer, PVME-*co*-MA-*co*-iPrMA, yielded stable dispersions of the particles (even after isolation), even though polydisperse in size. A schematic representation of the dispersion polymerization of acrylamide in TBA is given in Fig. 7. Note that emulsion and/or dispersion techniques have been employed depending upon the nature of the polymers employed.

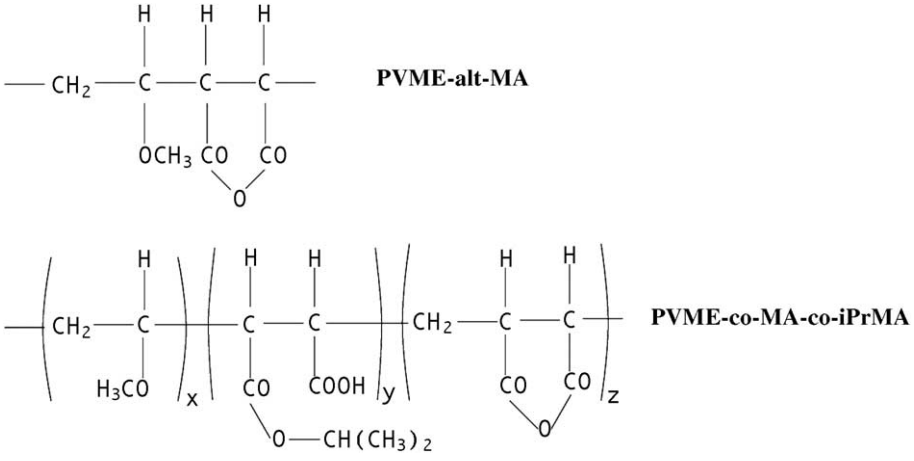

Fig. 7. Dispersion polymerization of acrylamide (reprinted from J. Colloid Interf. Sci. 271, S. Gubha, B. Mandal, Dispersion polymerization of acrylamide III. Partial isopropyl ester of poly(vinyl methyl ether-*alt*-maleic anhydride) as a stabilizer, 55–59 © 2004, with permission from Elsevier).

3.1.3. Interfacial polymerization/denaturation and desolvation

Nanoparticles can also be polymerized by interfacial polymerization and denaturation/desolvation for drug delivery to the CNS. Like emulsion polymerization, in interfacial polymerization, the monomers are used to create the solution. High-torque mechanical stirring brings the aqueous and organic phases together by emulsification or homogenization. Polyalkylcyanoacrylate NPs have been polymerized by this method. In addition, denaturation and desolvation have been used to produce the polymeric NPs. Lockman et al. gives a more detailed review of these procedures [53].

3.2. Nanoparticles and the BBB permeability

Koziara et al. have prepared the novel NPs, by warm microemulsion precursors, for transport across the BBB [54]. Two types of nanoparticles (emulsifying wax NPs/Brij 78 surfactant, and Brij 72 NPs/Tween-80 surfactant) were fabricated and radiolabelled by entrapment of [^{3}H]cetyl alcohol. The entrapment efficiency and release of the radiolabel were evaluated by an in situ rat brain perfusion method to determine the transport of NPs across the BBB. In the perfusion method, the animal's circulating blood is substituted with vascular perfusion fluid. Meanwhile, the in vivo constitution of the BBB and brain tissue is exploited. Briefly, buffered perfusion fluid (containing NaCl, Na_2PO_3 $NaHCO_3$, KCl, $CaCl_2$, $MgCl_2$, and D-glucose), with [^{3}H] NP and [^{14}C]sucrose (to determine the vascular volume), was infused into the left common carotid artery at a rate of 10 mL/min for periods of 15–60 s; the pressure in the carotid artery was maintained at ~120 mm Hg. Kinetics analyses were performed on the labeled NPs at the end of perfusion. The brain uptake of Brij 72 coated NPs was found higher than that observed for Brij 78 NPs, a fact attributed to the use of Tween-80 in the former polymerization. Moreover, [^{14}C] sucrose labeling verified the integrity of the BBB when it was found that the vascular space did not increase in the presence of nanoparticles. Lastly, the authors suggested endocytosis or transcytosis as possible mechanisms for transport; however, they have not elucidated these schemes.

Nanoparticles have also been used in the in vivo investigation of BBB permeability following cerebral ischemia and reperfusion. Fluorescent polystyrene NPs were injected intravenously into rats under ischemic attack. A microdialysis probe was implanted directly into the brains of the rats by stereotaxic injection. The nanoparticles were collected in the extracellular interstitial fluid by in vivo microdialysis; the presumption being that these particles were extravasated from the capillaries, and so therefore, represent permeability of the BBB (see Fig. 8). The cerebral oxygenation level was determined by oxygen-dependent quenching of phosphorescence of the nanoparticles. This was done to correlate the BBB permeability to extravasated NPs with oxygen concentration, following the cerebral ischemia and reperfusion. The induced ischemia was by the occlusion of the middle cerebral artery (MCA), and was followed by fluorescence intensity. Yang et al. found that this technique could be used to measure extracellular NPs in situ in the brain [55]. Under normal oxygen conditions, the NPs remained in the vasculature. However, MCA occlusion yielded an immediate increase in the extracellular concentration of the NPs. Subsequent fluorescent intensity in the microdialysate was resultant from the induced states of ischemia and reperfusion. This model represents the BBB permeability and so can be further probed as a system for drug delivery to the brain.

Oligonucleotides (ODN) are the negatively charged macromolecules that exhibit poor cellular uptake [56]. Their charge and size characteristics alone make them unsuitable for facile passage through the BBB. In addition, ODN have high renal clearances and are prone to enzymatic degradation, both in the systemic circulation [57] and by intracellular nucleases [54]. Examples of cationic carriers to improve the cellular uptake of ODN are reviewed in the literature [58–61]. Vinogradov et al. have encapsulated ODN within stable dispersions of cross-linked poly(ethylene glycol) (PEG) and polyethyleneimine ("nanogel") for the delivery of the macromolecule across the BBB [38,62]. The theory behind nanogels is that they are fabricated without the drug using the emulsification solvent evaporation method [32,63]. Afterwards, the nanogels are swollen in water to load the drug. Cationic cross-linked covalent chains of PEG and PEI spontaneously

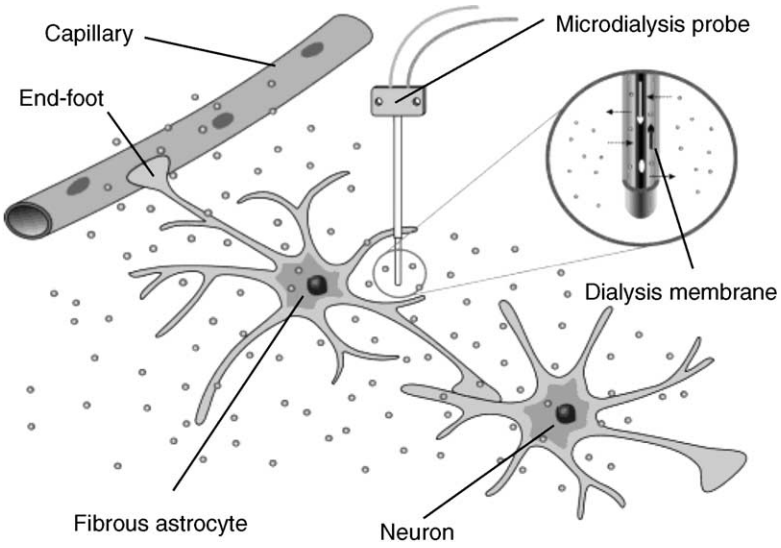

Fig. 8. Schematics of nanoparticles used to investigate BBB permeability by in vivo microdialysis following cerebral ischemia and reperfusion (reprinted with permission from C. Yang, C. Chang, P. Tsai, W. Chen, F. Tseng, L. Lo, Nanoparticle-based in vivo investigation on blood–brain barrier permeability following ischemia and reperfusion, Anal. Chem. 76 (2004) 4465–4471. Copyright 2004, Amer. Chem. Soc.).

encapsulate the negatively charged ODN. After drug loading, the solvent volume decreases and the gel collapses to form nanoparticles.

Nanogel was conjugated with biotin, and the biotinylated nanogel was subsequently labeled with rhodamine isothiocyanate (RITC). The ODN was labeled with fluorescein isothiocyanate (FITC) and with tritium for fluorescent and radiographic analysis. Nanogels were tritium labeled to aid in radiographic analysis upon in vivo biodistribution. To the solution of rhodamine labeled biotinylated ODN encapsulated nanogels, avidin and biotinylated bovine transferrin or biotinylated bovine insulin was added, to prepare the complex as vectors for drug delivery (see Fig. 9). Bovine brain microvessel endothelial cells (BBMEC) were isolated and grown as a polarized monolayer to mimic the BBB; transepithelial electrical resistance (TEER) values were recorded as a standard measure of the integrity of the monolayer. Transport studies were conducted by placing the BBMEC monolayers in side-by-side diffusion chambers. The donor chamber contained the nanogel–ODN dispersions with the paracellular diffusion marker ^{3}H-mannitol. Cellular accumulations of FITC–ODN and RITC–nanogel were accessed by confocal laser fluorescent microscopy of BBMEC cells grown on chamber slides. Finally, in vivo biodistribution studies were preformed by intravenous administration to wild type mice, using the ^{3}H-labeled compounds in the nanogel–ODN complex. After injection, organs were homogenized and the amounts of ^{3}H-nanogel or ^{3}H-ODN in the homogenate were measured by liquid scintillation.

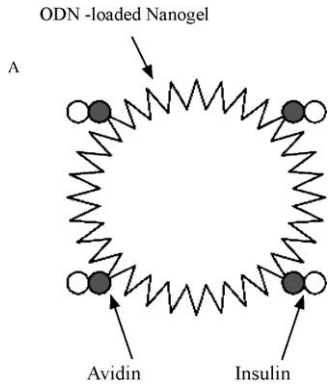

Fig. 9. Schematic representation of a vectorized nanogel, manipulated for in vivo brain delivery of oligonucleotides (ODN) (reprinted in part with permission from S. Vinogradov, E. Batrakova, A. Kabanov, Nanogels for oligonucleotide delivery to brain, Biocon. Chem. 15 (2004) 50–60. Copyright 2004, Amer. Chem. Soc.).

Vinogradov et al. found an 80% uptake of the ^{3}H-nanogel by the BBMEC [62]. The rate of transport of the drug-loaded nanogels was a function of the BBMEC complexes; positively charged complexes more efficiently transported the drug-loaded nanogels than did the negatively charged complexes. It was also found that the ODN transported with the nanogel to the BBMEC monolayer remained at least 2/3 bound in the receiver unit of the diffusion chamber. In addition, the layer was 6-fold more permeable to the nanogel–ODN as compared to the free ODN. The BBB permeability further increased by vectorizing the nanogels with the insulin and transferrin ligands (11- to 12-fold increases compared to the free ODN). Furthermore, the paracellular marker ^{3}H-mannitol was transported along with the nanogel–ODN complex in the diffusion chamber, suggesting a mechanism of transport at the BBB and verifying the integrity of the tight junctions of the monolayer.

Cytotoxicity of the nanogels was assessed, and conclusions were drawn that the complexes and complex compounds were nontoxic to the BBMEC monolayer, thus suggesting the potential of this carrier in the biological system. Uptake of the FITC–ODN and RITC–nanogels by the BBMEC was found mainly in the cytoplasm, although some FITC–ODN was localized in the nucleus. This suggested that a small portion of ODN released and transported to the nucleus since nanogels cannot penetrate the nuclear membrane due to size exclusion of the pores. The in vivo biodistribution studies exhibited high levels of free ODN in the liver and spleen, with increasingly smaller amounts in the brain. The nanogel–ODN complex, however, greatly increased the BBMEC permeability to ODN, with decreases in the liver and the spleen. Therefore, nanogels increased the brain uptake of the ODN and protected the macromolecule from rapid clearance by peripheral organs.

Lin et al. have prepared novel NPs by ionic gelation of poly-γ-glutamic acid (γ-PGA) into a hydrophilic, low-molecular weight (MW) chitosan (CS) solution; the application of the NPs to paracellular transport was investigated in an in vitro design by measuring the transepithelial electrical resistance (TEER) of Caco-2 cell monolayers [64]. TEER values are informative of the tightness of the junctions between the cells. Hence, decreased TEER values are expected when TJs open. The NPs were physicochemically characterized by Fourier transformed infrared (FTIR) spectroscopy, dynamic light scattering (DLS), transmission electron microscopy (TEM) and atomic force microscopy (AFM). Paracellular transport was visualized by confocal laser scanning microscopy (CLSM). The CS was depolymerized by enzymatic hydrolysis to produce the low-MW CS, which was characterized by gel permeation chromatography (GPC). Colonies of *Bacillus licheniformis* were cultured and grown to produce the γ-PGA, which was purified by centrifugation and dialysis, and confirmed by proton NMR (^{1}H NMR) and FTIR analyses. The NPs were obtained instantaneously, by mixing (by magnetic stirring) varying

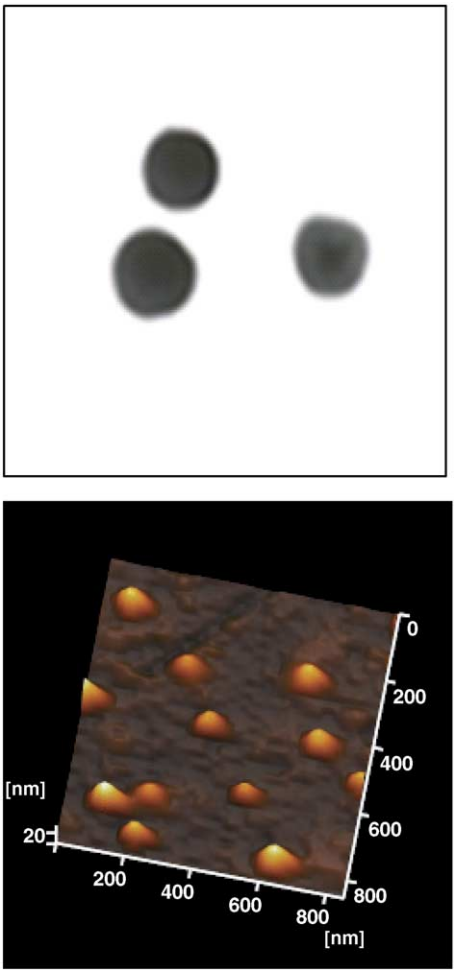

Fig. 10. TEM (0.10% γ-PGA:0.20% CS) and AFM (0.01% γ-PGA:0.01% CS). micrographs of CS-γ-PGA NPs (taken from [67]).

concentrations of aqueous solutions of the γ-PGA (pH 7.4) and the low-MW CS (pH 6.0), and were isolated by ultracentrifugation (38,000 rpm, 1 h). Morphology of the NPs was examined by TEM and AFM. The Caco-2 cells were cultured for use in the transport experiments. The cells were equilibrated with transport media, in which they were incubated along with the NPs, which were fluorescently labeled (with fluorescein isothiocyanate, FITC) (fCS-γ-PGA NP) for visualization by CLSM. This suspension was introduced into the donor compartment of the transport chamber, whereby the TEER values were monitored.

The authors found that the particle size and zeta potential of CS-γ-PGA NP could be controlled by their constituent components, thus ensuring stabilization of the NPs upon manipulation of the component concentrations [64]. In addition, stability studies of the positively (0.10% γ-PGA: 0.20% CS) and negatively (0.10% γ-PGA: 0.01% CS) surface charged NPs were performed, and no aggregation or precipitation of either (for up to 6 weeks) was reported. Fig. 10 shows the TEM and AFM results of the CS-γ-PGA NPs. A significant reduction in the TEER values of the Caco-2 cells was found upon incubation with the positively charged (CS dominated on the surface) NPs. In fact, the NPs with the positive surface charge reduced the TEER values of the Caco-2 cells by 50%, indicating that the TJs between the cells had been opened, presumably by chitosan. Moreover, when the incubated NPs were removed from the transport chamber, the TEER values of the Caco-2 cells increased (see Fig. 11), indicating recovery of the TJ. However, the NPs with a negative surface charge (γ-PGA dominated on the surface) did not significantly change the TEER values of the Caco-2 cells, as compared to the control (no NP incubation) group. These results indicate that the CS, and not the γ-PGA, opens the intercellular TJ, a phenomenon visualized by CLSM (see Fig. 12). By CLSM, fCS-γ-PGA NP transport through the Caco-2 cells was visualized at both incubation time and monolayer depth variables; fluorescence intensity was measured at 20 and 60 min of incubation with the NPs, and at depths of 0–15 μm from the apical surface of the monolayer. The authors, therefore, successfully verified the passive diffusion of NPs through the paracellular pathway [64].

It should be noted that Caco-2 is a human epithelial colorectal adenocarinoma cell line, and does not represent the endothelial cells required to study the properties of the BBB. However, integral and accessory proteins of the TJ are not unique between epithelial and endothelial cells, particularly the zona

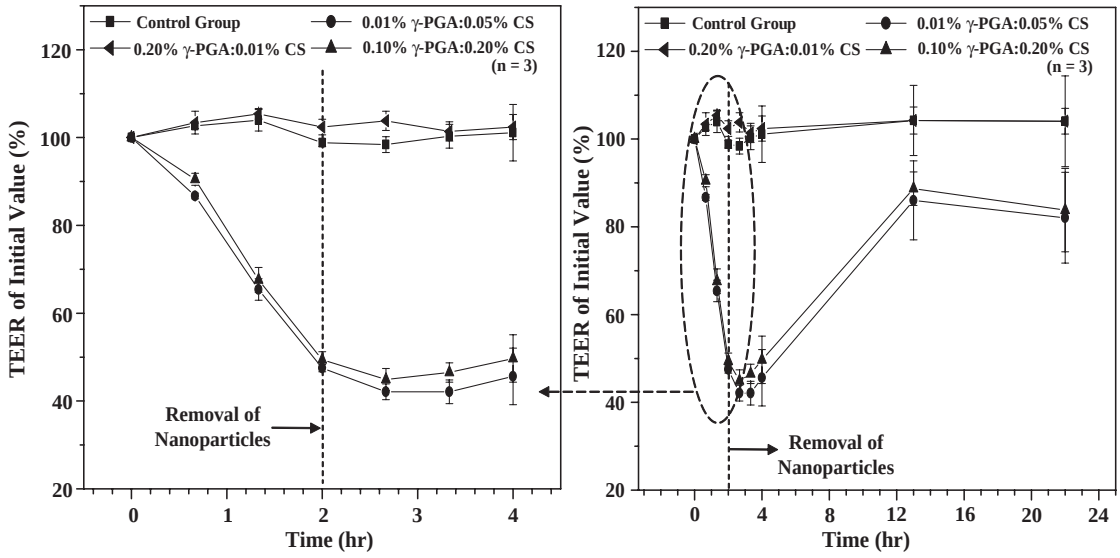

Fig. 11. Effect of CS-γ-PGA NPs on TEER values of Caco-2 cells. NPs with a positive surface charge have reduced the values of TEER. This suggests that CS-γ-PGA NPs can open intercellular tight junctions, thereby enhancing paracellular transport of ions, macromolecules and hydrophilic drugs (taken from [67]).

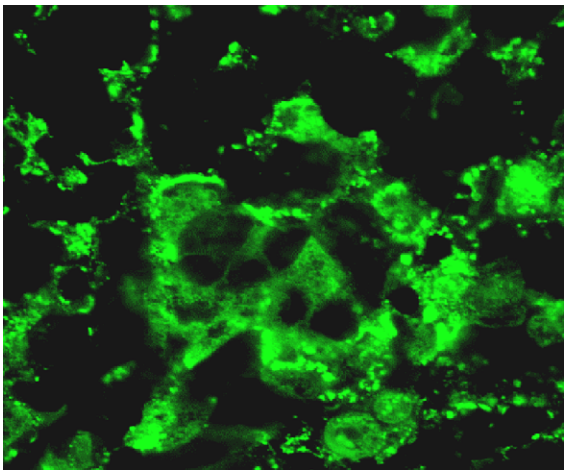

Fig. 12. Fluorescence image (taken by an inversed confocal laser scanning microscope) of an optical section (0 μm) of a Caco-2 cell monolayer that had been incubated with fCS-γ-PGA nanoparticles with a positive surface charge (0.10% γ-PGA: 0.20% CS) for 20 min (taken from [67]).

occludens protein, the protein implicated by Lin et al. [64], and its role on paracellular transport [7,15,18,20,21,23,65,66]. We therefore, hypothesize that the line of work undertaken by Lin et al. is applicable to the field of targeted drug delivery through the BBB [67]. Particularly, NPs can be chemically designed with the appropriate surface characteristics to cross the brain microvascular endothelial cells, and the physics of this occurrence verified by TEER (see Fig. 11). Biologically, the live cells can be visualized by CLSM (see Fig. 12), and at last, the NPs introduced into the murine model for the in vivo assessment of neurological disorders such as AD; these surveys are currently in progress.

Advances in the merging fields of BBB/CNS disorders and nanoparticle technology, such as vectorization, drug loading/release, etc., are widely covered in the literature [68]. For example, Garcia-Garcia et al. give an interesting review on using polymers as implantable intracerebral controlled-release devices to deliver drugs directly to brain interstitium in a sustained way [68]. By this method, the rates of drug transport, metabolism and elimination can be carefully upheld. Furthermore, Lockman et al. [69] have employed nanoparticles, surface-coated with a radiolabelled thiamine ligand, as a vector to the BBB in order to understand the in-situ brain perfusion of a rat [69]. The authors showed successful brain entry of the thiamine-coated nanoparticles [69]. Moreover, the thiamine associates with BBB transporters, thereby providing a possible explanation for the facilitation of NP-assisted drug delivery. In addition, solid lipid nanoparticles (SLN) have been investigated as drug vectors to the brain. For example, Wang et al. have found enhanced targeting, and subsequent increased brain uptake, of the drug 3′,5′-dioctanoyl-5-2′deoxyuridine (DO-FUdR) once it is incorporated into SLNs [70]. The authors achieved a nearly 30% drug loading efficiency, and the targeting efficiency to the brain was significantly increased from 11.77% to 29.81%, and with a prolonged half-life; SLNs improve the lipophilicity of the drug complex, thereby increasing the chances of the delivery of the incorporated drug across the BBB. Finally, NPs have been found to increase the BBB permeability of brain capillary endothelial cells (by transcytosis) when vectorized with cationic bovine serum albumin (CBSA) and poly(ethyleneglycol)–poly(lactide) (PEG–PLA) [71].

4. Alzheimer's disease

Alzheimer's disease results from the deposition of the amyloid beta protein (senile plaques) into the extracellular synaptic spaces of the neocortex, particularly in the temporal and parietal lobes. Neurodegeneration affects the cognition (learning, abstraction, judgment, etc.) and the memory with behavioral consequences such as aggression, depression, hallucination, delusion, anger and agitation [72]. Pathologically, ventricular enlargement and atrophy of the hippocampus (the limbic structure responsible for the memory) and the cerebral cortex can be seen. At present, the definitive diagnoses of AD are made upon histological verification of the Aβ plaques (or the hyperphyosphorlyated tau protein) at autopsy. The tau protein is normally seen in microtubule formation, but causes neurofibrillary tangles (NFT) in AD.

4.1. Genomics and proteomics of AD

The amyloid beta peptide is a normal metabolic byproduct of the amyloid precursor protein (APP). The gene encoding the amyloid precursor protein is located on chromosome 21, and it has been shown

that trisomy 21 (Down's syndrome) leads to the neuropathology of AD [73]. APP is normally cleaved by proteases called α-, β-, and γ-secretases, however, mutations along the gene encoding APP occur at these cleavage sites, eventually leading to the abnormal intramembranous processing of APP, and the consequential extracellular deposition of Aβ. Likewise, these mutations influence the self-aggregation of Aβ into amyloid fibrils [74]. In addition, the presenilin proteins (PS1 and PS2, located on chromosomes 14 and 1, respectively) have been found to alter the APP metabolism by the direct effect of γ-secretase [75]. Fagan et al. [76] have shown that the E4 isoform of the apolipoprotein E (chromosome 19) facilitates the formation of Aß fibrils in genetically engineered mice [76]. The collective effect of these processes is the increased production and accumulation of the (1–42) fragment of the amyloid beta peptide. The Aβ (1–42) oligomerizes and deposits in the synaptic space as diffuse plaques. The result is synaptic injury, preceded by the microgliagial activation, followed by oxidative stress, neuronal death, and dementia.

4.2. The metallochemistry of AD/oxidative stress

The Aβ peptide exists as three types in the brain: membrane-bound, aggregated (Aβ 1–42) and soluble (Aβ 1–40, found in biological fluids) [77]. Membrane bound Aβ is found in healthy individuals, while the aggregated and soluble peptide is located in the disease-affected individuals. The normal brain shows increased metallation upon aging; in AD, some of these metals are found at extremely high levels in the neocortical regions. In particular, the transition metals such as copper, iron and zinc are implicated in the neurotoxicity of the Aβ [78]. It is conjectured that a dyshomostasis, rather than toxological exposure to these ions, results in the pathogenesis of AD [79].

The Aβ is physiologically associated with Cu^{2+}, and copper is thought to aggregate [79] Aβ in acidic conditions. The AβCu^{2+} catalyzes [4] the generation of hydrogen peroxide (H_2O_2) [77] through the reduction of Cu^{2+} and Fe^{3+}, using oxygen and endogenous reducing agents. The H_2O_2 permeates the cell membranes, and if not broken down by catalyses, highly reactive hydroxyl radicals form (through the Fenton reaction), which disrupts the genetic material (DNA), and modifies proteins and lipids. In addition, apoptosis is induced by the permeation of H_2O_2 through the cell membrane [80]. Thus, the Aβ (1–42) has a higher binding affinity for copper than does the Aβ (1–40), which may account for the preferential aggregation of Aβ42 [79].

The neurochemistry of Aβ in the presence of iron is akin to that of copper. Namely, iron aggregates Aβ through redox chemistry-type reactions [79]. The Fenton reaction generates H_2O_2 production, as is similarly seen in the Aβ interactions with copper. Likewise, analogous fates of the protein transpire. Zinc exerts effects in the AD brain in a manner different than those put forth by copper and iron. First, zinc precipitates Aβ at the physiological pH, whereas copper and iron require mild acidic conditions [79]. Accordingly, the difference in pH accounts for a hastening of beta amyloid deposition by zinc. Yet another profound distinction classifying zinc from other metals is that it is redox-inert, and hence, inhibits the production of H_2O_2. Therefore, zinc's role in Aβ physiology is as that of an antioxidant. Zinc's inhibitory role in the production of H_2O_2 is attributed to the ion's competitive nature against copper for the Aβ binding sites [80]. However, zinc is not found concentrated enough in the brain to completely eliminate Aβ neurotoxicity [81].

5. Nanoparticles and Alzheimer's disease

5.1. Quinoline derivatives

Having been exploited in medicine as antibiotics, quinolines are effective against microbial diseases such as malaria [82]. The quinoline derivative viz., clioquinol (5-chloro-7-iodo-8-hydroxyquinoline,CQ) (shown in Fig. 13) is a Cu/Zn chelator known to

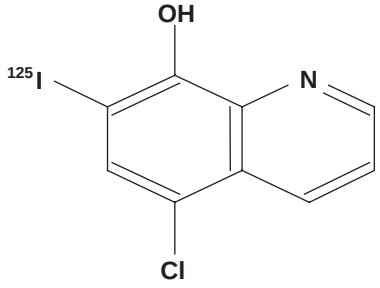

Fig. 13. Structure of ^{125}I-Clioquinol.

solubilize the Aβ plaques in vitro and inhibits the Aβ accumulation in AD transgenic mice in vivo [83]. Cherny et al. have validated these findings in their investigations of CQ for the treatment of AD [84]. In vitro assays showed that CQ dissolved Aβ (1–40) aggregates induced by Zn^{2+} or Cu^{2+}, but could not resolubilize the peptide at pH 5.5, which induces β-sheet formation. The binding interactions of CQ with Aβ were studied by NMR spectroscopy. The Aβ (1–28) is the histidine containing metal-binding fragment of Aβ, and was therefore, the selected fragment for spectroscopic study. NMR demonstrated that CQ removed bound Cu^{2+} from Aβ (1–28). NMR confirmed that CQ binds to the histidine residues, but not the peptide. Additionally, postmortem human AD brain homogenates were incubated with CQ and observed for the presence of peptide solubilization. Cherny et al. found that Aβ40 and Aβ42 were liberated in the soluble phase in the presence of CQ [5,77].

Aged APP2576 transgenic (Tg) mice with advanced Aβ deposition were treated with CQ for 9 weeks by oral administration. A decrease in the deposition of Aβ in the APP2576 Tg mouse upon treatment with CQ was observed. Additionally, serum levels of Aβ were significantly decreased in CQ treated animals compared to control, and there was a correlation between the serum Aβ and the cerebral Aβ. However, the authors [5,77] did not cite toxicity of CQ at the reported dose and CQ has neurological side effects, such as myelo-optic neuropathy, upon oral administration [84]. The toxicity has been attributed to vitamin B_{12} deficiency. Novel *n*-butylcyanoacrylate NPs have been fabricated with CQ encapsulated within the polymeric matrix. Particular emphasis could be placed on the prospects of CQ–NP as a vector for the in vivo brain imaging of Aβ senile plaques. Wadghiri et al. have performed in vivo brain imaging of APP Tg and APP/PS1 Tg mice using magnetically labeled Aβ (1–40), coupled with monocrystalline iron oxide nanoparticles (MION) coinjected with mannitol to transiently open the BBB [85]. However, in our scheme, the CQ–NP freely crosses the BBB, thus guaranteeing as unnecessary the additional use of intermediates, and therefore, reigning more feasible to the design process. In regards to Cherny's work [5,84], CQ–NP crosses the BBB at a higher threshold than CQ. Upon in vivo intravenous administration in the wild type mouse, the CQ–NP have greater brain uptake than the free drug alone. In accordance, we maintain that the CQ–NP delivery system can be used as a prototype in the treatment of AD.

In a continuing research on the development of novel NPs, Roney et al. have prepared the NPs by different polymerization techniques and performed the in vivo biodistribution to find an appropriate candidate for future in vivo imaging of amyloid beta plaques [86]. Briefly, the CQ was radioiodinated and incorporated within PBCA nanoparticles for the in vivo biodistribution in wild type Swiss webster mice (20–25 g). The NPs were polymerized as per the modified procedure of Kreuter et al. [48]. Briefly, an acidic polymerization medium containing Dextran 70,000 and Tween-80 (polysorbate 80) were used (both at a concentration of 1% each in 0.1 N HCl) (Sigma, USA). A 300×10^6 CPM ^{125}I-CQ was added to the solution just prior to the addition of butylcyanoacrylate (BCA) monomer. Butylcyanoacrylate 1% (Sichelwerke, Hannover, Germany) was added under constant magnetic stirring at 400 rpm. After 3 h of polymerization, the NP suspension was neutralized with 0.1 N NaOH to complete the polymerization. This solution was filtered with 0.2 μm filter and purified by ultracentrifugation (45 K rpm, 1 h). The pellet was washed and redispersed in water, which contained 1% Tween-80. The PBCA nanoparticles were then overcoated with 1% Tween-80 by stirring for 30 min in phosphate buffer solution (PBS), just before in vivo administration. A 1 mg of the nanoparticle was administered by intravenous injection and the particle size has been determined by a Zetasizer 3000 HS (Malvern, UK).

The R_h of the empty PBCA nanoparticles was 20 nm. After loading with Congo Red (CR), R_h=36.7 nm; PBCA nanoparticles when loaded with the amyloid affinity dye Thioflavin-S (ThS) had R_h=23.5 nm; PBCA nanoparticles loaded with amyloid affinity dye Thioflavin-T (ThT) had R_h=39.3 nm. Thus, drug loading of PBCA nanoparticles with amyloid dyes did not appreciably affect the sizes of the NPs. The PBCA NPs were successfully loaded with the radiolabelled quinoline derivatives ^{125}I-CQ and delivered to the mice by intravenous administration. The NPs were shown to successfully transport the drug across the BBB. The ^{125}I-CQ cleared the brain and blood, making this candidate ideal for in vivo imaging. Fig.

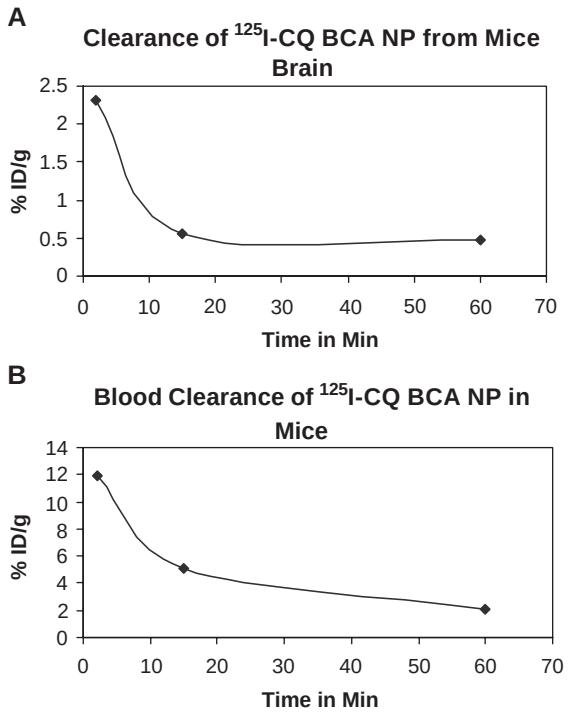

Fig. 14. Brain clearance of ^{125}I-CQ BCA NP in mice (A) and blood clearance of ^{125}I-CQ BCA NP in mice (B).

14 represents in vivo clearance of nanoparticles in the brain and the blood (Tables 3 and 4).

5.2. Thioflavin-T

The hydrophilic, charged, fluorescent marker Thioflavin-T (ThT) has been previously described as a probe for the detection of Aβ in senile plaques [87]. Hartig et al. delivered the encapsulated ThT NPs (of the butylcyanoacrylate polymer) into the mice brains by direct intrahippocampal injection, and followed the photoconversion of the ThT from the NPs in fixed tissues, post injection [87]. Core shell latex particles were synthesized by the emulsion polymerization of styrene in a water–ethanol mixture containing ThT. These particles were used in the seeded, aqueous polymerization of butylcyanoacrylate (BCA), which contained additional ThT in the polymerization media. The resulting core-shell NPs were administered to mice by stereotaxic injection into the hippocampus. The brains were fixed 3 days post injection, and the NPs were localized by photoconversion of the ThT in a closed chamber enriched with oxygen.

Table 3
Biodistribution of ^{125}I-CQ BCA nanoparticles in mice [86]

%ID/g	2 min	15 min	1 h
Blood	11.97 ± 2.78	5.06 ± 1.44	2.03 ± 1.15
Brain	2.31 ± 0.89	0.548 ± 0.06	0.48 ± 0.60
Liver	14.52 ± 1.98	8.63 ± 1.96	3.51 ± 1.88
Spleen	1.63 ± 0.47	1.56 ± 0.46	1.04 ± 0.99

Table 4
Biodistribution of ^{125}I-CQ in mice [86]

%ID/g	2 min	15 min	1 h
Blood	9.46 ± 2.88	2.63 ± 0.82	1.51 ± 0.65
Brain	1.14 ± 0.43	0.31 ± 0.01	2.64 ± 0.94
Liver	12.63 ± 1.29	3.67 ± 0.98	5.48 ± 0.61
Spleen	2.54 ± 0.16	1.41 ± 1.08	0.57 ± 0.36

Light microscopy localized photoconverted NPs in the dentate gyrus, and vacuoles were found in the cytoplasm near the aggregated latex nanoparticles. Transmission electron microscopy (TEM) verified the presence of NPs in microglia and neurons. Additionally, the high-powered TEM demonstrated that ThT was delivered from the NPs. As a result, the authors suggest that ThT core-filled latex particles can be used to probe the intracellular synthesis of Aβ, as well as its extracellular deposition [88]. They have not delivered these NPs to the brain through the systemic circulation; however, the chemical similarity of these NPs to butylcyanoacrylates, which have been shown to cross the BBB after intravenous administration [48], regards this promising approach as a potential Aβ detection method.

5.3. D-Penicillamine

The concentration of metal ions in the brain accumulates with age, the impact of which imparts lethal effects on the AD brain. Increases in the concentration of copper initiates oxidative stress, generating deadly hydroxyl radicals, which disrupts DNA and modifies proteins and lipids [89]. It is known that amyloid plaques contain the elevated levels of Cu (~400 μM) and Zn (~1 mM) compared to the healthy brain (70 μM Cu; 350 μM Zn) [90]. In an in vitro study of the chelation therapy for the possible treatment of AD, Cui et al. conjugated the Cu (I) chelator D-penicillamine to NPs to reverse the metal-induced precipitation of the beta amyloid protein [90]. Nanoparticles were

engineered from microemulsion precursors by melting the non-ionic emulsifying wax in the aqueous phase, before the addition of the surfactant, Brij 78. The microemulsion was cooled with a constant stirring to obtain the NPs, to which sodium salts of 1,2-dioleoyl-*sn*-glycero-3phosphoethanolamine-*N*-[4-(*p*-maleimidophenyl)butyramide] (MPB-PE) or 1,2 dioleoyl-*sn*-glycero-3-phosphoethanolamine-*N*-[3-(2-pyridyldithio)-propionate] (PDP-PE) were incorporated. The sulfhydryl moiety of D-penicillamine was coupled to the MPB-PE or PDP-PE nanoparticles in water, and under nitrogen gas with proper pH adjustments. Conjugation was measured by gel permeation chromatography (GPC). The stabilities of GPC-purified D-penicillamine conjugated PDP-nanoparticles were studied at 4° and 25 °C, and to salt as well as serum challenge, to determine the nature of the NPs in the biological environment. The Aβ (1–42) was induced to aggregate with $CuCl_2$, and samples were incubated with control (no chelator), EDTA (a metal chelator), D-penicillamine conjugated PDP-NPs, D-penicillamine, or PDP-NPs. The samples were centrifuged and the percent Aβ in the soluble fraction of the supernatant (% resolubilized) was calculated.

Nanoparticles of MPB-PE or PDP-PE conjugated with D-penicillamine were polymerized and fully characterized for aggregation, storage and pH sensitivity. The D-penicillamine conjugated to both MPB-PE or PDP-PE by the thioether and sulfydryl groups, respectively. Stability studies were performed with reducing agents on PDP-NP to determine if the –SH moiety could be cleaved (since it is less stable than the thioether bond of MPB-PE). Co-elution of the D-penicillamine with NPs on the GPC column verified conjugation, and NPs were stable under the tested conditions. It was found that the maximum amount of MPB-PE and PDP-PE that could be loaded onto NPs, while keeping the size <100 nm was 10% (w/w). At equimolar concentrations, the resolubilization of Aβ was 80% with EDTA and 40% with D-penicillamine, but at higher concentrations of D-penicillamine, resolubilization was just as effective. Importantly, the D-penicillamine conjugated to PDP-NPs did not resolubilize the peptide. However, after treating the NPs under basic conditions (and with increased temperature) to partially release the penicillamine, the plaques were solubilized by approximately 40%.

Cui et al. have shown that the NPs together with the partially released D-penicillamine resolubilized the plaques under reducing conditions [90]. They conducted % release studies of the penicillamine, but in an in vivo study, they would also need to perform the time release studies. In the in vivo system, they postulated glutathione to be the reducing agent to release the D-penicillamine from the NPs. The authors based this on the fact that glutathione is a highly concentrated non-protein thiol under normal physiological conditions that can participate in disulfide exchange. However, the authors did not explore the glutathione system, but they surmise the role of NPs in the in vivo investigation of AD through copper chelation [90].

6. Conclusions

Endothelial cells of the BBB limit the solute movement into the brain by regulating transport mechanisms at the cell surface. These transport mechanisms help to keep the harmful substances out of the brain in order to maintain homeostasis. However, the neurological disorders, such as Alzheimer's disease, can be elucidated if these barriers can be overcome or manipulated. Polymeric nanoparticles are the promising candidates to deliver drugs beyond the BBB for the scrutiny of the central nervous system. There are challenges ahead of us to resolve the question of binding of the drugs (loaded onto nanoparticles) to amyloid plaques. More research is in progress to address such challenging problems.

Acknowledgements

This work was supported by NIH F31 GM06638-03. The authors would like to thank Drs. Charles White and Dwight German for supply of brain tissue, and the UT Southwestern Medical Center Alzheimer's Disease Center (ADC) for support of this work. The authors would like to thank Dr. Michael Bennett for consultation. The investigations were conducted in conjunction with Cancer Imaging Program Pre-ICMC P20 CA086354. This report represents the research efforts under the triangular MoU between the University of Texas Southwestern Medical Center

at Dallas, the University of Texas at Dallas and Center of Excellence in Polymer Science, Karnatak University, Dharwad, India.

References

[1] R. Gutman, G. Peacock, D. Lu, Targeted drug delivery for brain cancer treatment, J. Control. Release 65 (2000) 31–41.
[2] Z. Zhuang, M. Kung, C. Hou, D. Skrovonsky, T. Gur, K. Plossl, J. Trojanoski, H. Kung, Radioiodinated styrylbenzenes and thioflavins as probes for amyloid aggregates, J. Med. Chem. 44 (2001) 1905–1914.
[3] Q. Smith, A Review of Blood Brain Barrier Transport Techniques, Humana Press, Inc., Totowa, NJ, 2003.
[4] X. Huang, M. Cuajungco, C. Atwood, Cu (II) potentiation of Alzheimer AB neurotoxicity, J. Biol. Chem. 274 (1999) 37111–37116.
[5] C. Ritchie, A. Bush, A. Mackinnon, S. Macfarlane, M. Mastwyk, L. MacGregor, L. Kiers, R. Cherny, Q. Li, A. Tammer, D. Carrington, C. Mavros, I. Volitakis, M. Xilinas, D. Ames, S. Davis, K. Beyreuther, R. Tanzi, C. Masters, Metal–protein attenuation with iodochlorhydorxyquin (clioquinol) targeting AB amyloid deposition and toxicity in Alzheimer disease, Arch. Neurol. 60 (2003) 1685–1691.
[6] T. Reese, M. Karnovsky, Fine structural localization of a blood–brain barrier to exogenous peroxidase, J. Cell Biol. 34 (1967) 207–217.
[7] S. Nag, Morphology and Molecular Properties of Cellular Components of Normal Cerebral Vessels, Humana Press, Totowa, NJ, 2003.
[8] Q. Yan, E. Sage, Transforming growth factor-beta 1 induces apoptotic death in cultured retinal endothelial cells but not in pericytes: association with decreased expression of p21 wafl/cip1, J. Cell. Biochem. 70 (1998) 70–83.
[9] K. Hirshi, P. D'Armore, Control of angiogenesis by pericytes: molecular mechanisms and significance, EXS 79 (1997) 419–428.
[10] C. Johanson, Permeability and vascularity of the developing brain: cerebellum vs. cerebral cortex, Brain Res. 190 (1980) 3–16.
[11] W. Pardridge, Molecular Biology of the Blood–Brain Barrier, Humana Press, Totowa, NJ, 2003.
[12] C. Crone, S. Olesen, Electrical resistance of brain microvascular endothelium, Brain Res. 241 (1982) 49–55.
[13] D. Krause, U. Mischeck, H. Galla, R. Dermietzel, Correlation of zonua occludens ZO-1 antigen and transendothelial resistance in porcine and rat cultured cerebral endothelial cells, Neurosci. Lett. 128 (1991) 301–304.
[14] Q. Smith, S. Rapoport, Cerebrovascular permeability coefficients to sodium, potassium and chloride, J. Neurochem. 46 (1986) 1732–1742.
[15] M. Furuse, T. Hirase, M. Ito, Occludin: a novel integral membrane protein localizing at tight junctions, J. Cell Biol. 123 (1993) 1777–1788.
[16] H. Wolburg, A. Lippoldt, Tight junctions of the blood–brain barrier: development, composition and regulation, Vasc. Pharmacol. 38 (2002) 323–337.
[17] H. Wolburg, K. Wolburg-Bucholz, J. Kraus, G. Rascher-Eggstein, S. Liebner, S. Hamm, F. Duffner, E.-H. Grote, W. Risau, B. Engelhardt, Localization of claudin-3 in tight junctions of the blood–brain barrier is selectively lost during experimental autoimmune encephalomyelitis and human glioblastoma multiforme, Acta Neuropathol. 105 (2003) 586–592.
[18] I. Martin-Padura, S. Lostaglio, M. Schneemann, Junctional adhesion molecule, a novel member of the immunoglobulin superfamily that distributes at intercellular junctions and modulates monocyte transmigration, J. Cell Biol. 142 (1998) 117–127.
[19] K. Morita, H. Sasaki, M. Furuse, S. Tsukita, Endothelial claudin: claudin-5/TMVCF constitutes tight junction strands in endothelial cells, J. Cell Biol. 147 (1999) 185–194.
[20] L. Mitic, C.V. Itallie, J. Anderson, Molecular physiology and pathophysiology of tight junctions, Am. J. Physiol.: Gasterointest. Liver Physiol. 279 (2000) G250–G254.
[21] M. Furuse, K. Fujimoto, N. Sato, T. Hirase, S. Tsukita, S. Tsukita, Overexpression of occludin, a tight junction integral membrane protein, induces the formation of intracellular multilamellar bodies bearing tight junction-like structures, J. Cell. Sci. 109 (1996) 429–435.
[22] L. Mitic, J. Anderson, Molecular architecture of tight junctions, Annu. Rev. Physiol. 60 (1998) 121–142.
[23] A. Reichel, D. Begley, N. Abbott, in: S. Nag (Ed.), Methods in Molecular Medicine: The Blood–Brain Barrier: Biology and Research Protocols, Humana Press, Inc., Totowa, NJ, 2003, pp. 307–325.
[24] A. Ring, J. Weiser, E. Tuomanen, Pneumococcal trafficking across the blood–brain barrier: molecular analysis of a novel bidirectional pathway, J. Clin. Invest. 102 (1998) 347–360.
[25] B. Pron, M. Taha, C. Rambaud, J. Fournet, N. Pattey, J. Monnet, M. Musilek, J. Beretti, X. Nassif, Interaction of Neisseria meningitidis with the components of the blood–brain barrier correlates with an increased expression of PilC, J. Infect. Dis. 176 (1997) 1285–1292.
[26] E. Neuwelt, Mechanisms of disease: the blood–brain barrier, Neurosurgery 54 (2004) 131–141.
[27] J. Huber, K. Witt, S. Hom, R. Egleton, K. Mark, T. Davis, Inflammatory pain alters blood–brain barrier permeablility and tight junctional protein expression, Am. J. Physiol. 280 (2001) H1241–H1248.
[28] Q. Smith, in: E. Neuwelt (Ed.), Implications of the Blood Brain Barrier and its Manipulation, Plenum Press, New York, 1989, pp. 85–118.
[29] G. Lee, S. Dallas, M. Hong, R. Bendayan, Drug transporters in the central nervous system: brain barriers and brain parenchymal considerations, Pharmacol. Rev. 53 (2001) 569–596.
[30] A. Kabanov, E. Batrakova, New technologies for drug delivery across the blood–brain barrier, Curr. Pharm. Des. 10 (2004) 1355–1363.
[31] J. Kreuter, in: J.B.J. Swarbrick (Ed.), Encyclopedia of Pharma. Tech., Marcel Dekker, New York, 1994, pp. 165–190.

[32] S.A. Agnihotri, N.N. Mallikaujuana, T.M. Aminabhavi, Recent advances on chitosan-based micro and nanoparticles in drug delivery, J. Control. Release 100 (2004) 5–28.
[33] T.M. Aminabhavi, K.S. Soppimath, A.R. Kulkarni, W.E. Rudzinski, Biodebradable polymeric nanoparticles as drug delivery devices, J. Control. Release 70 (2001) 1–20.
[34] N. Behan, C. Birkinshaw, N. Clarke, Poly *n*-butyl cyanoacrylate nanoparticles: a mechanistic study of polymerization and particle formation, Biomaterials 22 (2001) 1335–1344.
[35] H. Fessi, F. Puisieux, J. Devissaguet, N. Ammoury, S. Benita, Nanocapsule formation by interfacial polymer deposition following solvent displacement, Int. J. Pharm. 55 (1989) R1–R4.
[36] S. Gubha, B. Mandal, Dispersion polymerization of acrylamide, J. Colloid Interface Sci. 271 (2004) 55–59.
[37] J. Leroux, E. Allemann, E. Doelker, R. Gurnay, New approach for the preparation of nanoparticles by an emulsification–diffusion method, Eur. J. Pharm. Biopharm. 41 (1995) 14–18.
[38] Y. Li, Y. Pei, Z. Zhou, X. Zhang, Z. Gu, J. Ding, J. Zhou, X. Gao, PEGylated polycyanoacrylate nanoparticles as tumor necrosis factor-alpha carriers, J. Control. Release 73 (2001) 287–296.
[39] R. Lobenberg, L. Araujo, H. Briesen, E. Rodgers, J. Kreuter, Body distribution of azidothymidine bound to hexyl-cyanoacrylate nanoparticles after i.v. injection to rats, J. Control. Release 50 (1998) 21–30.
[40] H. Murakami, M. Yoshino, M. Mizobe, M. Kobayashi, H. Takeuchi, Y. Kawashima, Preparation of poly(D,L-lactide-co-glycolide) latex for surface modifying material by a double coacervation method, Proc. Int. Symp. Control. Release Bioact. Mater. 23 (1996) 361–362.
[41] T. Niwa, H. Takeuchi, T. Hino, N. Kunou, Y. Kawashima, Preparations of biodegradable nanospheres of water-soluble and insoluble drugs with D,L-lactide/glycolide copolymer by a novel spontaneous emulsification solvent diffusion method and the drug release behavior, J. Control. Release 25 (1993).
[42] M. Peracchia, C. Vauthier, D. Desmaele, A. Gulik, J. Dedieu, M. Demoy, J. d'Angelo, P. Couvreur, PEGylated nanoparticles from a novel MePEGcyanoacrylate hexadecylcyanoacrylate amyphiphilic copolymer, Pharm. Res. 15 (1998) 548–554.
[43] G. Quintanar, Q. Ganem, E. Allemann, G. Fessi, Influence of the stabilizer coating layer on the purification and freeze drying of poly (D,L-lactic acid) nanoparticles prepared by the emulsification–diffusion technique, J. Microencapsul. 15 (1998) 107–119.
[44] P. Scholes, A. Coombes, L. Illum, S. Davis, M. Vert, M. Davies, The preparation of sub-500 nm poly(lactide-co-glycolide) microspheres for site-specific drug delivery, J. Control. Release 25 (1993) 145–153.
[45] P. Wehrle, P. Magenheim, S. Benita, Influence of process parameters on the PLA nanoparticle size distribution evaluated by means of factorial design, J. Pharm. Biopharm. 41 (1995) 19–26.
[46] M. Zambaux, F. Bonneaux, R. Gref, P. Maincent, E. Dellacherie, M. Alonso, P. Labrude, C. Vigernon, Influence of experimental parameters on the characteristics of poly(lactic acid) nanoparticles prepared by double emulsion method, J. Control. Release 50 (1998) 31–40.
[47] J. Kreuter, Nanoparticulate systems for brain delivery of drugs, Adv. Drug Deliv. Rev. 47 (2001) 65–81.
[48] J. Kreuter, R. Alyautdin, D. Kharkevich, A. Ivanov, Passage of peptides through the blood–brain barrier with collodial polymer particles (nanoparticles), Brain Res. 674 (1995) 171–174.
[49] U. Schroeder, P. Sommerfeld, B. Sabel, Efficacy of oral dalargin-loaded nanoparticle delivery across the blood–brain barrier, Peptides 19 (1998) 777–780.
[50] U. Schroeder, B. Sabel, H. Schroeder, Diffusion enhancement of drugs by loaded nanoparticles in vitro, Prog. Neuro-Psychopharmacol. Biol. Psychiatry 23 (1999) 941–949.
[51] C. Vauthier, C. Dubernet, C. Chauvierre, I. Brigger, P. Couvreur, Drug delivery to resistant tumors: the potential of poly (alkyl cyanoacrylate) nanoparticles, J. Control. Release 93 (2003) 151–160.
[52] P. Munk, T.M. Aminabhavi, Introduction to Macromolecular Science, John Wiley & Sons, Inc., New York, 2002.
[53] P. Lockman, R. Mumper, M. Khan, D. Allen, Nanoparticle technology for drug delivery across the blood–brain barrier, Drug Dev. Ind. Pharm. 28 (2002) 1–13.
[54] J. Koziara, P. Lockman, D. Allen, R. Mumper, In situ blood–brain barrier transport of nanoparticles, Pharm. Res. 20 (2003) 1772–1778.
[55] C. Yang, C. Chang, P. Tsai, W. Chen, F. Tseng, L. Lo, Nanoparticle-based in vivo investigation on blood–brain barrier permeability following ischemia and reperfusion, Anal. Chem. 76 (2004) 4465–4471.
[56] W. Broaddus, C. Prabhu, S. Wu-Pong, G. Gillies, H. Fillmore, Strategies for the design and delivery of antisense oligonucleotides in central nervous system, Methods Enzymol. 314 (2000) 121–135.
[57] S. Yang, L. Lu, Y. Cai, J. Zhu, B. Liang, C. Yang, Body distribution in mice of intravenously injected campothecin solid lipid nanoparticles and targeting effect on brain, J. Control. Release 59 (1999) 299–307.
[58] O. Boussif, F. Lezoualc'h, M. Zanta, M. Mergny, D. Scherman, B. Demeneix, J. Behr, A versatile vector for gene and oligonucleotide transgene into cells in culture and in vivo: polyethylenimine, Proc. Natl. Acad. Sci. U. S. A. 92 (1995) 7297–7303.
[59] J. Jeong, S. Kim, T. Park, A new antisense oligonucleotide delivery system based on self-assembled ODN–PEG hybrid conjugate micelles, J. Control. Release 93 (2003) 183–191.
[60] J. Kim, B. Kim, A. Maruyama, T. Akaike, S. Kim, A new nonviral DNA delivery vector: the terplex system, J. Control. Release 53 (1998) 175–182.
[61] O. Meyer, D. Kirpotin, K. Hong, B. Sternberg, J. Park, M. Woodlei, D. Papahadjopoulos, Cationic liposomes coated with polyethylene glycol as carriers for oligonucleotides, J. Biol. Chem. 25 (1998) 15621–15627.
[62] S. Vinogradov, E. Batrakova, A. Kabanov, Poly(ethyleneglycol)-[polyethyleneimine NanoGel particles: novel drug delivery systems for antisense oligonucleotides, Colloids Surf., B Biointerfaces 16 (1999) 291–304.
[63] K.S. Soppimath, A.R. Kulkarni, T.M. Aminabhavi, Chemically modified polyacrylamide-g-guar gum based cross-linked anionic microgels as pH-sensitive drug delivery systems: pre-

paration and characterization, J. Control. Release 75 (2001) 331–345.
[64] Y.-H. Lin, C.K. Chung, C.T. Chen, H.F. Liang, S.C. Chen, H.W. Sung, Preparation of nanoparticles composed of chitosan/poly-Á-glutamic acid and evaluation of their permeability through Caco-2 cells, Biomacromolecules 6 (2005) 1104–1112.
[65] M. Furuse, K. Fujita, T. Hiiragi, K. Fujimoto, S. Tsukita, Claudin-1 and -2: novel integral membrane protein localizing at tight junctions, J. Cell Biol. 141 (1998) 1539–1550.
[66] C. Chavany, T. Doan, P. Couvreur, F. Puisieux, C. Helene, Polyalkylcyanoacrylate nanoparticles as polymeric carriers for antisense oligonucleotides, Pharm. Res. 9 (1992) 441–449.
[67] Y.-H. Lin, C.K. Chung, C.-T. Chen, H.-F. Liang, S.-C. Chen, H.W. Sung, Preparation of nanoparticles composed of chitosan/poly-r-glutamic acid and evaluation of their permeability through Caco-2 cells, Biomacromolecules 6 (2005) 1104–1112.
[68] E. Garcia-Garcia, K. Andrieux, S. Gil, P. Couvreur, Collodial carriers and blood–brain barrier (BBB) translocation: a way to deliver drugs to the brain? Int. J. Pharm. 298 (2005) 274–292.
[69] P. Lockman, M. Oyewumi, J. Koziara, K. Roder, R. Mumper, D. Allen, Brain uptake of thiamine-coated nanoparticles, J. Control. Release 93 (2003) 271–282.
[70] J.-X. Wang, X. Sun, Z.-R. Zhang, Enhanced brain targeting by synthesis of 3′,5′-diocyanoyl-5-fluoro-2′-deoxyuridine and incorporation into solid lipid nanoparticles, Eur. J. Pharm. Biopharm. 54 (2002) 285–290.
[71] W. Lu, Y.-Z. Tan, K.-L. Hu, X.-G. Jiang, Cationic albumin conjugated pegylated nanoparticle with its transcytosis ability and little toxicity against blood–brain barrier, Int. J. Pharm. 295 (2005) 247–260.
[72] M. Olson, C. Shaw, Presenile dementia and Alzheimer's disease in mongolism, Brain 92 (1969) 147.
[73] J. Hardy, D. Selkoe, The amyloid hypothesis of Alzheimer's disease: progress and problems on the road to therapeutics, Science 297 (2002) 353–356.
[74] D. Walsh, D. Selkoe, Deciphering the molecular basis of memory failure in Alzheimer's disease, Neuron 44 (2004) 181–193.
[75] M.S. Wolfe, Presenilin and gamma-secretase: structure meets function, J. Neurochem. 76 (2001) 1615–1620.
[76] A. Fagan, M. Watson, M. Parasadanian, K. Bales, S. Paul, D. Holtzman, Human and murine ApoE markedly alters Abeta metabolism before and after plaque formation in a mouse model of Alzheimer's disease, Neurobiol. Dis. 9 (2002) 305–318.
[77] T. Lynch, R. Cherny, A. Bush, Oxidative process in Alzheimer's disease. The role of AB–metal interactions, Exp. Neurol. 35 (2000) 445–451.
[78] A. Finefrock, A. Bush, M. Doraiswamy, Current status of metals as therapeutic targets in Alzheimer's disease, J. Am. Geriatr. Soc. 51 (2003) 1143–1148.
[79] A. Bush, The metallobiology of Alzheimer's disease, Trends Neurosci. 26 (2003) 207–214.
[80] C. Opazo, X. Huang, R.A. Cherny, R.D. Moir, A.E. Roher, A.R. White, Metalloenzyme-like activity of Alzheimer's disease β-amyloid: Cu-dependent catalytic conversion of dopamine, cholesterol and biological reducing agents to neurotoxic H_2O_2, J. Biol. Chem. 277 (2002) 40302–40308.
[81] M.P. Cuajungco, L.E. Goldstein, A. Nunomura, M.A. Smith, J.T. Lim, C.S. Atwood, Evidence that the beta-amyloid plaques of Alzheimer's disease represent the redox-silencing and entombent of AB by zinc, J. Biol. Chem. 275 (2000) 19439–19442.
[82] R. Brueckner, T. Coster, D. Wescher, M. Shmuklarsky, B. Schuster, Prophylaxis of Plasmodium flaciparum infection in a human challenge model with WR 238605, a new 8-aminoquinoline antimalarial, Antimicrob. Agents Chemother. 42 (1998) 1293–1294.
[83] X. Huang, C.S. Atwood, M.A. Hartshorn, G. Multhaup, L.E. Goldstein, R.C. Scarpa, The AB peptide of Alzheimer's disease directly produces hydrogen peroxide through metal ion reduction, Biochemistry 38 (1999) 7609–7616.
[84] R.A. Cherney, C.S. Atwood, M.E. Xilinas, D.N. Gray, W.D. Jones, C.A. McLean, Treatment with a copper–zinc chelator markedly and rigidly inhibits B-amyloid accumulation in Alzheimer's disease transgenic mice, Neuron 30 (2001) 665–676.
[85] Y. Wadghiri, E. Sigurdsson, M. Sadowski, J. Wlliott, Y. Li, H. Scholtzova, C. Tang, G. Aguinaldo, M. Pappolla, K. Duff, T. Wizniewski, D. Turnbull, Detection of Alzheimer's amyloid in transgenic mice using magnetic mice using magnetic resonance microimaging, Mag. Res. Med. 50 (2003) 293–302.
[86] C. Roney, V. Arora, P. Kulkarni, M. Bennett, P. Antich, F. Bonte, Unpublished data.
[87] W. Hartig, B. Paulke, C. Varga, J. Seeger, T. Harkany, J. Kacza, Electron microscopic analysis of nanoparticles delivering thioflavin-T after intrahippocampal injection in mouse: implications for targeting β-amyloid in Alzheimer's disease, Neurosci. Lett. 338 (2003) 174–176.
[88] J. Dong, C. Atwood, V. Anderson, S. Siedlak, M. Smith, G. Perry, P. Carey, Metal binding and oxidation of amyloid-beta within isolated senile plaque cores: Raman microscopic evidence, Biochemistry 42 (2003) 2768–2773.
[89] M. Lovell, J. Robertson, W. Teesadale, J. Campbell, W. Markesbery, Copper, iron and zinc in Alzheimer's disease senile plaques, J. Neurol. Sci. 158 (1998) 47–52.
[90] Z. Cui, P. Lockman, C. Atwood, C. Hsu, A. Gupte, D. Allen, R. Mumper, Novel D-penicillamine carrying nanoparticles for metal chelation therapy in Alzheimer's and other CNS diseases, Eur. J. Pharm. Biopharm. 59 (2005) 263–272.